Algebraic Geometrization of the Kuramoto Model: Equilibria and Stability Analysis

Dhagash Mehta,[1, *] Noah S. Daleo,[2, †] Florian Dörfler,[3, ‡] and Jonathan D. Hauenstein[1, §]

[1]*Dept. of Applied and Computational Mathematics and Statistics,*
University of Notre Dame, Notre Dame, IN 46556, USA.
[2]*Dept. of Mathematics, North Carolina State University, Raleigh, NC 27695, USA.*
[3]*Automatic Control Laboratory, Swiss Federal Institute of Technology (ETH) Zürich, 8092 Zürich, Switzerland.*

Finding equilibria of the finite size Kuramoto model amounts to solving a nonlinear system of equations, which is an important yet challenging problem. We translate this into an algebraic geometry problem and use numerical methods to find all of the equilibria for various choices of coupling constants K, natural frequencies, and on different graphs. We note that for even modest sizes ($N \sim 10 - 20$), the number of equilibria is already more than 100,000. We analyze the stability of each computed equilibrium as well as the configuration of angles. Our exploration of the equilibrium landscape leads to unexpected and possibly surprising results including non-monotonicity in the number of equilibria, a predictable pattern in the indices of equilibria, counter-examples to popular conjectures, multi-stable equilibrium landscapes, scenarios with only unstable equilibria, and multiple distinct extrema in the stable equilibrium distribution as a function of the number of cycles in the graph.

Introduction. - The Kuramoto model is a fascinating model proposed in 1975 to study synchronization phenomena [1] that has gained attention from various scientific communities, including biology, chemistry, physics, and electrical engineering, due to its applicability. This model has been used to study various phenomena including neural networks, chemical oscillators, Josephson junctions and laser arrays, power grids, particle coordination, spin glass models, and rhythmic applause [2–4].

The Kuramoto model is defined as a system of autonomous ordinary differential equations as:

$$\frac{d\theta_i}{dt} = \omega_i - \frac{K}{N} \sum_{j=1}^{N} a_{i,j} \sin(\theta_i - \theta_j), \text{ for } i = 1, ..., N, \quad (1)$$

where K is the coupling strength, N is the number of oscillators, $\Omega = (\omega_1, \ldots, \omega_N)$ is the vector of intrinsic natural frequencies, and $a_{i,j} \in \{0, 1\}$ is the (i,j)th element of the adjacency matrix of the coupling graph. The natural frequencies ω_i indicate how the system oscillates in the absence of any dissipation or exogenous forces.

The equilibrium conditions are $\frac{d\theta_i}{dt} = 0$ for all i. This system of equations has an $O(2)$ freedom, i.e., for any $\alpha \in (-\pi, \pi]$, the equations are invariant under replacing all θ_i with $\theta_i + \alpha$. This rotational symmetry leads to a continua of equilibria. To remove this $O(2)$ freedom resulting in finitely many equilibria, we fix one of the angles, say, $\theta_N = 0$, and remove the equation $\frac{d\theta_N}{dt} = 0$ from the system. The remaining system consists of $N-1$ nonlinear equations in $N-1$ angles.

Provided the coupling strength K is strong enough, the oscillators will synchronize as $t \to \infty$. In this setup, a critical coupling $K_c(N)$ exists at which the number of stable equilibria switches from 0 to a nonzero value. In the special case of $N \to \infty$ and long-range (all-to-all) coupling $a_{ij} = 1$, one may analytically compute $K_c(N)$. However, for the finite size Kuramoto model, such an

analysis may turn out to be very difficult. In particular, finding all equilibria, analyzing stability, and finding $K_c(N)$ is known to be prohibitively difficult for a finite but large oscillator population.

We point out that the equilibria of system (1) can also be viewed as the stationary points of the potential energy landscape drawn by the mean-field XY model with an exogenous perturbation term:

$$V(\theta) = \frac{K}{2N} \sum_{i,j=1}^{N} a_{i,j}(1 - \cos(\theta_i - \theta_j)) - \sum_{i=1}^{N} \omega_i \theta_i, \quad (2)$$

whose gradient reproduces the right-hand side of equation (1). Hence, in the following, we use the words equilibria and stationary points interchangeably.

All stationary points of the finite N mean-field XY model (i.e., the Kuramoto model with homogeneous frequencies) were identified in Ref. [5]. Building on Ref. [5], all stationary points of the one-dimensional nearest-neighbour XY model (i.e., the Kuramoto model with local coupling) for any given N with either periodic or anti-periodic boundary conditions have been found [6–9].

Using these solutions, a class of stationary points of the 2-dimensional nearest-neighbour XY model [10] and the XY model with long-range interactions [11] were built and analysed (see also [12, 13]). In Ref. [6, 7, 12, 14], all of the stationary points for small lattices were found using algebraic geometry methods. Bounds on the number of equilibria [15] as well as some counterintuitive examples to plausible conjectures [16] have been reported for the same model in the domain of power systems.

In Ref. [5] for the finite N mean-field XY model, and in Refs. [6, 10] for the nearest neighbour XY models, it was shown that there were exponentially many isolated stationary solutions as N increases. Moreover, even after breaking the global $O(2)$ symmetry, there were continuous solutions at the maximum value of the energy which

were independently observed and termed as *incoherent manifolds* in Ref. [17].

In Refs. [18–20], necessary and sufficient conditions are given for fixed points to exist for the finite size Kuramoto model for complete and bipartite graphs, and explicit upper and lower bounds of $K_c(N)$ for these systems were also computed, followed by providing an algorithm to compute $K_c(N)$. For the complete graph, similar results were presented in [21, 22], where it was additionally shown that there is exactly one single stable equilibrium for $K > K_c(N)$. In Ref. [23], an analogous result was shown for acyclic graphs, short cycles, and complete graphs as well as combinations thereof. In the case of homogeneous natural frequencies networks with sufficiently high nodal degrees, the only stable fixed point is known to be the phase-synchronized solution [24]. In Ref. [25], all of the stable synchronized states were classified for the one-dimensional Kuramoto model on a ring graph with random natural frequencies in addition to computing a lower bound on $K_c(N)$ (see also Ref. [42, 43]).

Algebraic Geometry Interpretation and Setup. - We initiate an approach to study the Kuramoto model by using an algebraic geometry interpretation of the equilibria and studying synchronization. Upon fixing $\theta_N = 0$, we use the identity $\sin(x - y) = \sin x \cos y - \sin y \cos x$ and substitute $s_i = \sin \theta_i$ and $c_i = \cos \theta_i$ to transform the $N - 1$ equations into polynomials that are coupled by the Pythagorean identity $s_i^2 + c_i^2 = 1$. This results in a system of $2(N - 1)$ polynomials in $2(N - 1)$ variables:

$$\begin{aligned} 0 &= \omega_i + \frac{K}{N} \sum_{j=1}^{N} a_{i,j} \left(s_i c_j - s_j c_i \right) \\ 0 &= s_i^2 + c_i^2 - 1 \end{aligned} \quad (3)$$

Given a fixed integer N, our first goal is to find all real solutions of polynomial system (3) for a given choice of Ω, K, and adjacency matrix $A = [a_{ij}]$. We accomplish this using a technique from numerical algebraic geometry via parameter homotopies, which we briefly review below. Once the system is solved, we determine which solutions (if any) are stable steady-state solutions by analyzing the eigenvalues of the Jacobian at each real solution.

Numerical Algebraic Geometry Methods. - For a fixed N, we can interpret (3) as the system $F_N(s, c; K, \Omega, A) = 0$ with variables s and c and parameters K, Ω, and A. This leads to using parameter homotopies [26] for solving, which is a two-step process. First, in the *ab initio* phase, one computes all solutions for a sufficiently random set of parameters. Then, in the parameter homotopy phase, one solves for given parameters by deforming from the parameters selected in the *ab initio* phase. The *ab initio* phase is performed once, while the parameter homotopy phase is performed for each set of parameters. The following provides a short introduction with more details provided in [27, Ch. 7] and [28, Ch. 6].

This process is a generalization of other standard homotopy methods, such as a *total degree homotopy* or

multi-homogeneous homotopy frequently used, e.g., [27, 28, 31–39]. The method has also recently used in solving the power-flow systems [29, 30] For example, consider solving a system of m polynomial equations in m variables, $f(x) = (f_1(x), \ldots, f_m(x)) = 0$ where $x = (x_1, \ldots, x_m)$. For a total degree homotopy, the space of interest is the space of all polynomial systems $g(x)$ of m polynomials in m variables where $d_i := \deg f_i = \deg g_i$. Since a random element in this space has the Bézout number of roots, namely $\prod_{i=1}^{m} d_i$, the system $G = (G_1, \ldots, G_m) = \mathbf{0}$ where $G_i(x) = x_i^{d_i} - 1$ is sufficiently random in this space.

In this case, the *ab initio* phase for solving $G = 0$ is trivial. Then, in the parameter homotopy phase, one can consider the homotopy $H(x, t) = (1 - t)f(x) + \gamma t G(x)$ for a random $\gamma \in \mathbb{C}$. Now, the solutions of $H(x, t) = 0$ at $t = 1$ are known and we want to compute the solutions of $H(x, 0) = 0$. Using a numerical predictor-corrector method implemented in `Bertini` [40], we track each of the solution paths from $t = 1$ to $t = 0$. The number γ ensures that such path tracking will obtain *all* of the isolated complex solutions of $f(x) = 0$, from which the real and nonreal solutions can be identified.

Now, returning to our case F_N, suppose, for simplicity, that we want to study the behavior of the solutions of $F_N = 0$ as a function of K, that is, we also fix Ω and A. In the *ab initio* phase, we pick a random $K = K_0 \in \mathbb{C}$ and compute the solutions S_0 of $F_N(s, c; K_0, \Omega, A) = 0$ using a total degree homotopy described above via `Bertini`.

In the parameter homotopy phase, we consider solving for various choices of parameters K, e.g., $K = 2, \ldots, 100$. For each choice of K, we simply track the solution paths of $F_N(s, c; K \cdot (1 - t) + t \cdot K_0, \Omega, A) = 0$ starting at $t = 1$ with solutions S_0. Each of these computations is relatively inexpensive, thereby making it practical to compute the solutions at hundreds of different choices for K.

The resulting solutions are sorted based on whether they are real or not, and their stability is investigated as follows. From the sine s_i and cosine c_i values, we compute the corresponding angle θ_i. The eigenvalues of the Jacobian of (1) are used to analyze stability. The *index* is the number of positive eigenvalues so that real solutions with index zero correspond to stable steady states.

Results for the complete graph. - We start with the most prominent and well studied case corresponding to the complete graph, namely $a_{i,j} = 1$. We select $\Omega = (\omega_1 \ldots \omega_N)$ to be N equidistant numbers, namely $\omega_i = -1 + (2i - 1)/N$. Figures 1 and 2 summarize the number of real-valued solutions to the polynomial system (3) for $N = 3, \ldots, 18$ at various values of K. In general, we see that the number of distinct real solutions tends to grow as K increases. However, there are some surprising exceptions to this expected monotinicity property, e.g., the $N = 9$ case has 328 real solutions at $K = 60$ and 326 real solutions at $K = 70$. Our results suggest that eventually the number of real solutions stabilizes to
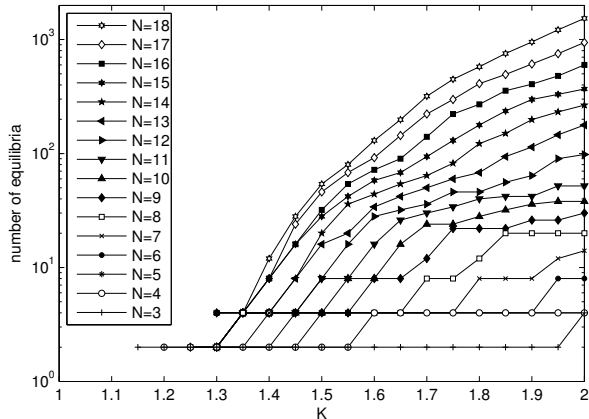
Figure 1. Number of equilibria for the case of equidistant natural frequencies on the complete graph at $1 \leq K \leq 2$.
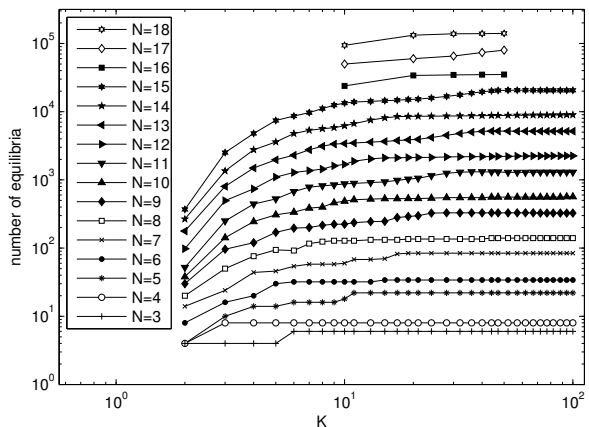

Figure 2. Number of equilibria for the case of equidistant natural frequencies on the complete graph at $2 \leq K \leq 100$.

a constant for each N. For $N = 18$, we computed 140,356 real solutions when $K = 50$; computing these without our polynomial formulation would be very difficult.

Once the real solutions are found, we turn our attention to determining which ones are stable. Via Jacobian analysis we find that there is exactly a single stable steady state solution for $N = 3, \ldots, 18$ at each K value tested, with the exception of small values of K which result in no real solutions. This result is consistent with theoretic findings for the complete graph [19–22]. Next, for each N we use the results of our stability analysis to determine numerical upper and lower bounds on $K_c(N)$ as follows. We acquire an upper bound on $K_c(N)$ by determining the smallest tested value of K for which a real steady state is found. Similarly, we find a lower bound on $K_c(N)$ by determining the largest tested value of K for which no real steady states are found. These results are presented in Figure 3. We verify that these bounds

for $K_c(N)$ are consistent with the known explicit bounds from [4, Corollary 6.7]. For $N \in \{3, 4\}$, our computed lower bound is less than the explicit lower bound due to the coarse resolution of tested numeric values for $K_c(N)$.
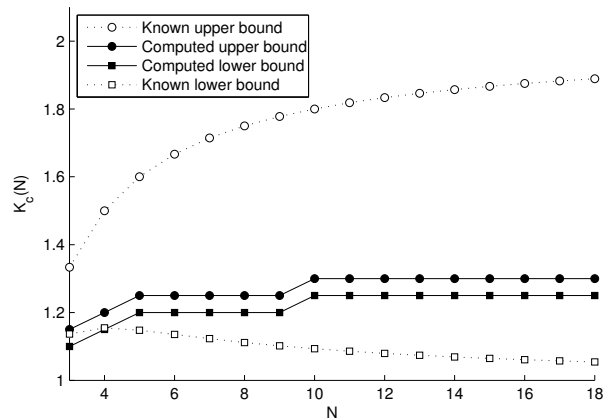

Figure 3. Bounds for $K_c(N)$ in the case of equidistant natural frequencies on the complete graph. Known explicit bounds from [4, Corollary 6.7] are shown for comparison.

In Ref. [16], it is conjectured that if there is a stable equilibrium, then there is a stable equilibrium satisfying $|\theta_i - \theta_j| < \pi/2$ for all neighbors $\{i, j\}$. We checked this conjecture and we quickly found counterexamples. For $N = 3$ and $K = 1.15$, there is one stable equilibria at $(\theta_1, \theta_2, \theta_3) \approx (1.6820, 0.8410, 0)$. Since θ_1 and θ_3 are coupled with $|\theta_1 - \theta_3| > \pi/2$, we reject the conjecture.

For larger N, the unique stable equilibria can have angles even more spread out, such as $(\theta_1, \ldots, \theta_{15}) \approx (2.0981, 1.8867, \ldots, 0.2114, 0)$ when $N = 15$ and $K = 1.3$. These interesting numerical observations prompt us to analytically reject the conjecture in [16]: in [4] it is shown that the worst-case equilibrium configuration for $K = K_c$ and $n > 3$ corresponds to a tripolar distribution of all angles spanning a half-circle. From [21, 22], we know that this is the only stable equilibrium. These two arguments suffice to reject the conjecture in [16].

As mentioned earlier, our stability analysis is based on computing the index corresponding to each real solution. Figure 4 shows a histogram of these values for the case $K = 100$. We observe that when j is small enough relative to N, the number of real solutions with index j is exactly $\binom{N}{j}$. In particular, for $3 \leq N \leq 4$ this behavior occurs for $j \leq 1$ and, for $5 \leq N \leq 18$, this behavior occurs for $j \leq \lceil \frac{2}{5}(N - 1) \rceil$. Based on these results, we conjecture that this phenomenon occurs in general: for equidistant natural frequencies, if $0 \leq j \ll N$ and $K \gg 0$, then the number of equilibria with index j is expected to be $\binom{N}{j}$. This conjecture can be used when N may be too large to compute all solutions. For example, we expect 75,287,520 real equilibria of index 5 for $N = 100$.

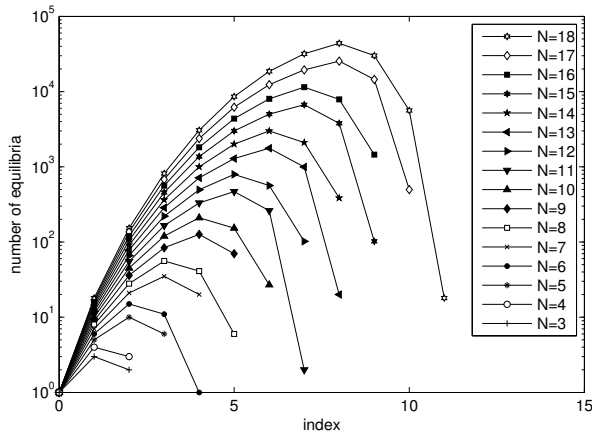*Results for cyclic graphs.* - Although our investigation

Figure 4. Number of equilibria with given index for equidistant natural frequencies and a complete graph with $K = 100$.

initially focused on the complete graph being the most well studied case, we also performed a preliminary analysis of the coupling arrangement defined by an undirected cyclic graph. Cyclic graphs are known for having multi-stable equilibria [4], entirely unstable equilibrium landscapes [16], and thus a quite distinct behavior from acyclic or complete graphs [23, 41, 43].

For $N = 10$, we used the same equidistant natural frequencies mentioned earlier with Figure 5 showing the number of equilibria and the number of stable equilibria at each integer $K = 0, \ldots, 100$.
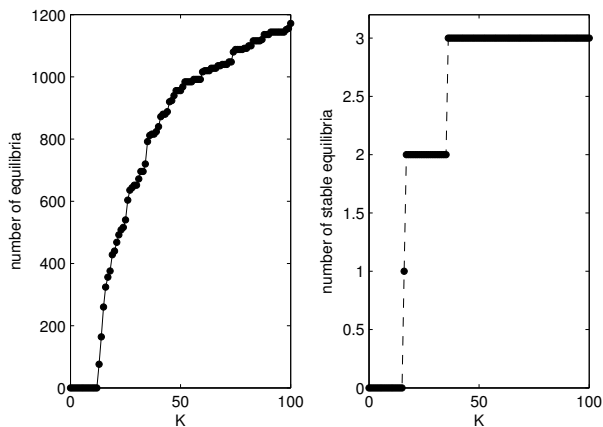

Figure 5. Number of equilibria and number of stable equilibria for a cyclic coupling arrangement when $N = 10$.

For some values of K, the system possesses only unstable equilibria. In particular, when K is 13, 14, or 15, there are 76, 164, and 260 equilibria, respectively, all of which are unstable. Since the critical points of the potential (2) correspond to power flow in a transmission network, a very interesting technological implication of these results is that there are power demands which can

be met only with unstable equilibria. We find one stable equilibria at $K = 16$ and conclude $15 \leq K_c(10) \leq 16$. Figure 5 also indicates multistability for some values of K, with at most *three* stable equilibria for each investigated sample. These results are in contrast to the complete graph case, in which exactly one stable equilibria exists whenever the system has real-valued solutions.

Next, we take a closer look at the geometric configuration of angles occurring at the stable equilibria shown in Figure 5. For relatively small K such as $K = 16, 17, 18$, the configuration of angles at stable equilibria shows no discernible structure. For $K = 35$ there are two stable equilibria, with one exhibiting phase sync, i.e., angles clustered around 0, and one exhibiting a splay state, i.e., angles approximately uniformly distributed on $[0, 2\pi)$. For the splay state, the θ_i decrease on $[0, 2\pi)$.

For each $K = 36, \ldots, 100$ there are three stable equilibria, with each case consisting of one phase sync and two splay states. In one of these splay states $\theta_1, \ldots, \theta_9$ are arranged in increasing order on $[0, 2\pi)$, and in the other $\theta_9, \ldots, \theta_1$ are arranged in decreasing order on $[0, 2\pi)$. In Figure 6, we depict the three stable equilibria at $K = 100$. As K increases, the steady state phase sync gradually becomes more tightly clustered, with the angle range decreasing from ~ 0.9432 for $K = 35$ to ~ 0.3256 for $K = 100$. This is in accordance with the asymptotic result that exact phase sync is a critical point of the Kuramoto potential (2) as $K \to \infty$ [4].
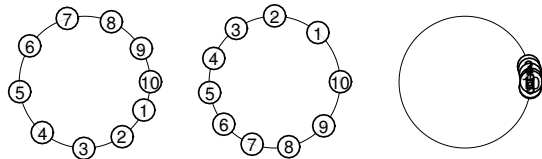

Figure 6. Configuration of $\theta_1, \ldots, \theta_{10}$ for the three stable equilibria occurring at $K = 100$ for a cyclic graph with $N = 10$.

Results for random graphs. - We now turn our attention to random coupling arrangements. In these computations, we choose each $a_{i,j}$ as 0 or 1 according to a pre-determined probability P while setting $a_{j,i} = a_{i,j}$. In other words, $[a_{i,j}]$ is the adjacency matrix of a symmetric Erdös-Rényi random graph with coupling probability P, where we restrict ourselves to connected graphs. For these numerical experiments, we use the same equidistant natural frequencies discussed earlier.

First, we fix $N = 8$ and $K = 100$ and investigate the number of stable equilibria for sparse random graphs. For each $c = 0, 1, \ldots, 20$, we construct 100 random graphs having exactly c cycles. We achieve this by generating adjacency matrices of symmetric Erdős-Rényi random graphs until we have 100 instances of connected graphs with the desired number of cycles. Depending on the graph, we find 1, 2, or 3 stable equilibria. The averages

of these results are shown in Figure 7 showing that the sparsest (i.e., acyclic) as well as sufficiently dense graphs have exactly one stable equilibrium confirming the analytic results for these two extremal topologies [4, 21–24]. Since cycles are known to display multi-stability (see Figure 5), it is to be expected that there is more than one stable equilibrium for small cycle numbers. Quite surprisingly, multiple distinct extrema can be observed in the stable equilibrium distribution in Figure 7.
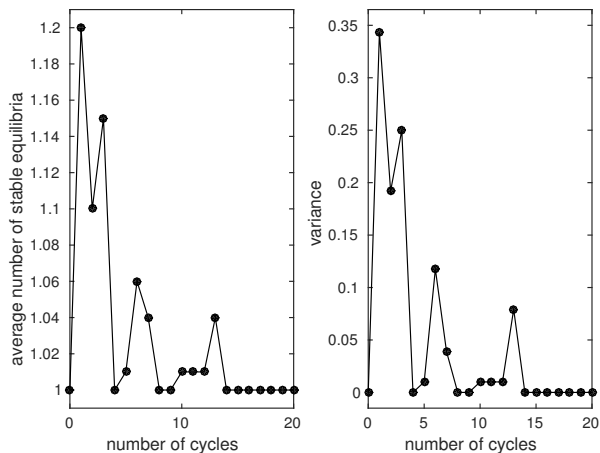

Figure 7. Number of stable equilibria for random graphs according to number of cycles in the case of $N = 8$ and $K = 100$.

Next, we fix $N = 10$ and investigate how $K_c(N)$ depends on the density of the graph. For each coupling probability $P = 0.25, 0.375, \ldots, 0.875$, we generated 100 random graphs. For each graph, we computed equilibria and determine stability at the following values of K: for $P = 0.25$ we use $K = 1, \ldots, 20$; for $P = 0.375$ we use $K = 1, \ldots, 15$; for $P = 0.5$ we use $K = 1, \ldots, 10$; and for each $P = 0.625, 0.75, 0.875$, we use $K = 1, \ldots, 5$. In all cases, we find a value of K such that at least one stable equilibrium occurs at K while no stable equilibria occur at $K - 1$, thereby allowing us to estimate bounds on $K_c(10)$. Figure 8 shows these results sorted according to the number of cycles in the graph.

For undirected and connected graphs, a theoretic lower and a conjectured theoretic upper bound are [4, 23]

$$N \cdot \max_i \left\{ \frac{|\omega_i|}{\deg_i} \right\} \leq K_c(N) \leq N \cdot \|B^T L^\dagger \omega\|_\infty,$$

where $\deg_i = \sum_j a_{ij}$ is the degree of node i, B is the oriented incidence matrix, and L is the network Laplacian matrix. These bounds are shown in Figure 8 for comparison. We verified that our 600 individual results as well as the averages shown are consistent with these theoretic bounds and validate their accuracy. Figure 8 indicates that the numerical upper bound is tighter than the theoretic bound on average, while the numerical lower bound

tends to be weaker. Since the tightness of our computed bounds depends on the resolution of K values tested, one could check more refined K values to obtain tighter numerical bounds for particular graphs of interest.
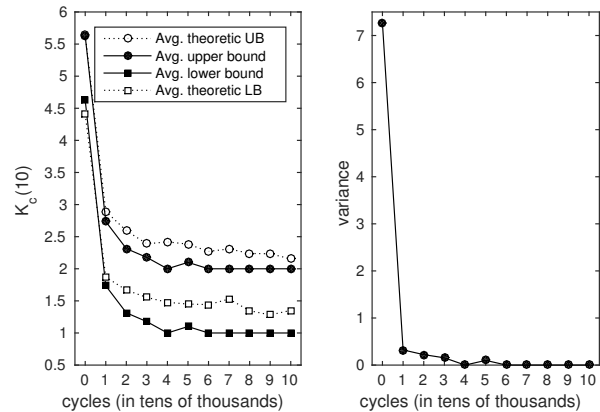

Figure 8. Average bounds on $K_c(N)$ for random graphs according to number of cycles in the case of $N = 10$.

Conclusion. - We have interpreted the problem of finding all of the equilibria of the Kuramoto model as an algebraic geometry problem by translating the stationary equations into a system of polynomial equations. The coupling constant, natural frequencies, and entries of the adjacency matrix of the corresponding graph can all be viewed as parameters of the system. With this unification, we show that the polynomial homotopy continuation method combined with parameter homotopies can not only find *all* isolated equilibria at each parameter point, but can also scan over a large set of parameters without having to re-solve the system at each instance.

For complete graphs, we find unexpected non-monotonicity in the number of equilibria as K increases. Our stability analysis leads us to a conjecture regarding the expected number of equilibria of certain index. Our investigation of angle configuration at steady states leads us to reject a conjecture from Ref. [16]. For cyclic graphs, we note certain coupling constants K result in only unstable equilibria, and we show multi-stable scenarios with a multi-modal stable equilibrium distribution depending on the number of cycles. Our experiments on random graphs shed insight into the Kuramoto model in a broader sense and show the importance of the coupling probability. All of our results are consistent with the available theoretic bounds which are quite loose at times.

Perhaps more importantly for complex systems areas, with the algebraic geometry interpretation and computational methods, we have developed a reliable and direct way of computing the critical coupling $K_c(N)$ for synchronization in the finite size Kuramoto model that does not rely on any specific frequency distribution or graph

topology. We are in the process of writing a more specific algorithm to compute $K_c(N)$ up to an arbitrary precision based on the algebraic geometry interpretation and parameter homotopy computations. In future work, we aim to extend our investigations to directed graphs, negative weights, cosine coupling, and statistical properties of random graph models, as well as verify conjectures for variations of the Kuramoto models as studied in Ref. [41].

---

* dmehta@nd.edu
† nsdaleo@ncsu.edu
‡ dorfler@ethz.ch
§ hauenstein@nd.edu

[1] Y. Kuramoto. Self-entrainment of a population of coupled non-linear oscillators. In *International symposium on mathematical problems in theoretical physics*, pages 420–422. Springer, 1975.

[2] J.A. Acebrón, L.L. Bonilla, C.J. Pérez Vicente, F. Ritort, and R. Spigler. The Kuramoto model: A simple paradigm for synchronization phenomena. *Reviews of modern physics*, 77(1):137, 2005.

[3] S.H. Strogatz. From Kuramoto to Crawford: exploring the onset of synchronization in populations of coupled oscillators. *Physica D: Nonlinear Phenomena*, 143(1):1–20, 2000.

[4] F. Dörfler and F. Bullo. Synchronization in complex oscillator networks: A survey. *Automatica*, 50(6):1539–1564, June 2014.

[5] L. Casetti, M. Pettini, and E.G.D. Cohen. Phase transitions and topology changes in configuration space. *Journal of Statistical Physics*, 111:1091–1123(33), June 2003.

[6] D. Mehta. Lattice vs. Continuum: Landau Gauge Fixing and 't Hooft-Polyakov Monopoles. *Ph.D. Thesis, The Uni. of Adelaide, Australasian Digital Theses Program*, 2009.

[7] D. Mehta and M. Kastner. Stationary point analysis of the one-dimensional lattice Landau gauge fixing functional, aka random phase XY Hamiltonian. *Annals Phys.*, 326:1425–1440, 2011.

[8] L. von Smekal, D. Mehta, A. Sternbeck, and A.G. Williams. Modified Lattice Landau Gauge. *PoS*, LAT2007:382, 2007.

[9] L. von Smekal, A. Jorkowski, D. Mehta, and A. Sternbeck. Lattice Landau gauge via Stereographic Projection. *PoS*, CONFINEMENT8:048, 2008.

[10] R. Nerattini, M. Kastner, D. Mehta, and L. Casetti. Exploring the energy landscape of XY models. *Phys.Rev.*, E87(3):032140, 2013.

[11] M. Kastner. Stationary-point approach to the phase transition of the classical xy chain with power-law interactions. *Physical Review E*, 83(3):031114, 2011.

[12] C. Hughes, D. Mehta, and J.-I. Skullerud. Enumerating Gribov copies on the lattice. *Annals Phys.*, 331:188–215, 2013.

[13] D. Mehta and M. Schröck. Enumerating copies in the first gribov region on the lattice in up to four dimensions. 2014.

[14] D. Mehta, A. Sternbeck, L. von Smekal, and A.G. Williams. Lattice Landau Gauge and Algebraic Geometry. *PoS*, QCD-TNT09:025, 2009.

[15] J. Baillieul and C.I. Byrnes. Geometric critical point analysis of lossless power system models. *IEEE Transactions on Circuits and Systems*, 29(11):724–737, 1982.

[16] A. Araposthatis, S. Sastry, and P. Varaiya. Analysis of power-flow equation. *International Journal of Electrical Power & Energy Systems*, 3(3):115–126, 1981.

[17] S.H. Strogatz and R.E. Mirollo. Stability of incoherence in a population of coupled oscillators. *Journal of Statistical Physics*, 63(3-4):613–635, 1991.

[18] M. Verwoerd and O. Mason. On computing the critical coupling coefficient for the Kuramoto model on a complete bipartite graph. *SIAM Journal on Applied Dynamical Systems*, 8(1):417–453, 2009.

[19] M. Verwoerd and O. Mason. Global phase-locking in finite populations of phase-coupled oscillators. *SIAM Journal on Applied Dynamical Systems*, 7(1):134–160, 2008.

[20] F. Dörfler and F. Bullo. On the critical coupling for kuramoto oscillators. *SIAM Journal on Applied Dynamical Systems*, 10(3):1070–1099, 2011.

[21] D. Aeyels and J.A. Rogge. Existence of partial entrainment and stability of phase locking behavior of coupled oscillators. *Progress on Theoretical Physics*, 112(6):921–942, 2004.

[22] R.E. Mirollo and S.H. Strogatz. The spectrum of the locked state for the Kuramoto model of coupled oscillators. *Physica D: Nonlinear Phenomena*, 205(1-4):249–266, 2005.

[23] F. Dörfler, M. Chertkov, and F. Bullo. Synchronization in complex oscillator networks and smart grids. *Proceedings of the National Academy of Sciences*, 110(6):2005–2010, 2013.

[24] R. Taylor. There is no non-zero stable fixed point for dense networks in the homogeneous Kuramoto model. *Journal of Physics A: Mathematical and Theoretical*, 45(5):055102, 2012.

[25] J. Ochab and P.F. Góra. Synchronization of coupled oscillators in a local one-dimensional Kuramoto model. *arXiv preprint arXiv:0909.0043*, 2009.

[26] A.P. Morgan and A.J. Sommese. Coefficient-parameter polynomial continuation. *Appl. Math. Comput.*, 29(2):123–160, 1989.

[27] A.J. Sommese and C.W. Wampler. *The Numerical Solution of Systems of Polynomials Arising in Engineering and Science.* World Scientific Publishing, Hackensack, NJ, 2005.

[28] D.J. Bates, J.D. Hauenstein, A.J. Sommese, and C.W. Wampler. *Numerically solving polynomial systems with Bertini*, volume 25. SIAM, 2013.

[29] D. Mehta, H. Nguyen, and K. Turitsyn, "Numerical Polynomial Homotopy Continuation Method to Locate All The Power Flow Solutions," *ArXiv e-prints*, 2014.

[30] S. Chandra, D. Mehta, and A. Chakrabortty, "Exploring the impact of wind penetration on power system equilibrium using a numerical continuation approach," *arXiv preprint arXiv:1409.7844*, 2014.

[31] D. Mehta. Numerical Polynomial Homotopy Continuation Method and String Vacua. *Adv.High Energy Phys.*, 2011:263937, 2011.

[32] M. Maniatis and D. Mehta. Minimizing Higgs Potentials via Numerical Polynomial Homotopy Continuation. *Eur.Phys.J.Plus*, 127:91, 2012.

[33] M. Kastner and D. Mehta. Phase Transitions Detached from Stationary Points of the Energy Landscape. *Phys.Rev.Lett.*, 107:160602, 2011.

[34] D. Mehta, Y.-H. He, and J.D. Hauenstein. Numerical Algebraic Geometry: A New Perspective on String and Gauge Theories. *JHEP*, 1207:018, 2012.

[35] D. Mehta, J.D. Hauenstein, and M. Kastner. Energy-landscape analysis of the two-dimensional nearest-neighbor ϕ^4 model. *Phys. Rev. E*, 85:061103, Jun 2012.

[36] B. Greene, D. Kagan, A. Masoumi, D. Mehta, E.J. Weinberg, and Xiao Xiao. Tumbling through a landscape: Evidence of instabilities in high-dimensional moduli spaces. *Phys.Rev.*, D88(2):026005, 2013.

[37] D. Mehta, D.A. Stariolo, and M. Kastner. Energy landscape of the finite-size spherical three-spin glass model. *Phys.Rev.*, E87(5):052143, 2013.

[38] D. Martinez-Pedrera, D. Mehta, M. Rummel, and A. Westphal. Finding all flux vacua in an explicit example. *JHEP*, 1306:110, 2013.

[39] Y.-H. He, D. Mehta, M. Niemerg, M. Rummel, and A. Valeanu. Exploring the Potential Energy Landscape Over a Large Parameter-Space. *JHEP*, 1307:050, 2013.

[40] D.J. Bates, J.D. Hauenstein, A.J. Sommese, and C.W. Wampler. Bertini: Software for numerical algebraic geometry. Available at `http://bertini.nd.edu`.

[41] D. A. Wiley, S. H. Strogatz and M. Girvan. Chaos: An Interdisciplinary J. of Non. Sci., **16** 015103 (2006).

[42] S. H. Strogatz and R. E. Mirollo. Physica D: Non. Phen., **31**, 143 (1988).

[43] G. B. Ermentrout. J. Math. Bio.,**23** 55 (1985).